

RAL 92029
Copy 1 R61
ACCN: 215089
RAL-92-029

Science and Engineering Research Council

Rutherford Appleton Laboratory

Chilton DIDCOT Oxon OX11 0QX

RAL-92-029

***** RAL LIBRARY R61 *****
ACC_No: 215089
Shelf: RAL 92029
R61

Spin Fluctuations in Heisenberg Magnets: Dynamic Critical Phenomena and Excitations in Quasi-Periodic Systems

S W Lovesey

LIBRARY, R61
-1 JUN 1992
RUTHERFORD APPLETON
LABORATORY

April 1992

Science and Engineering Research Council

"The Science and Engineering Research Council does not accept any responsibility for loss or damage arising from the use of information contained in any of its reports or in any communication about its tests or investigations"

**SPIN FLUCTUATIONS IN HEISENBERG MAGNETS:
DYNAMIC CRITICAL PHENOMENA AND EXCITATIONS IN
QUASI-PERIODIC SYSTEMS**

STEPHEN W LOVESEY
Rutherford Appleton Laboratory
Oxfordshire, OX11 0QX, UK

Prepared for: *Frontiers of Solid State Sciences*,
edited by L C Gupta and M S Multani (World Scientific)

SPIN FLUCTUATIONS IN HEISENBERG MAGNETS: DYNAMIC CRITICAL PHENOMENA AND EXCITATIONS IN QUASI-PERIODIC SYSTEMS

STEPHEN W LOVESEY
Rutherford Appleton Laboratory
Oxfordshire, OX11 0QX, UK

1. Prologue
2. Response Functions
3. Basic Concepts in Critical Phenomena
4. Coupled-Mode Calculations of $S(\mathbf{k}, \omega)$
 - 4.1 *Analytic Results*
 - 4.2 *Numerical and Experimental Results*
5. Muon Spin Relaxation: Antiferromagnetic Exchange
6. Quasi-Periodic Magnets
7. Analytic Expression for the Response Function of a Quasi-Periodic Magnet
8. Examples of the Response Function Including the Influence of Collision Damping
1. **Prologue**

The two main topics addressed in this article are dynamic critical phenomena, and spin excitations in a modulated (quasi-periodic) structure. In both cases, discussions are couched in terms of a Heisenberg model, which is appropriate for magnetic salts and adequate for rare earth and transition metal elements and alloys.

The topics share a number of features. First, the basic theoretical problems are in both cases examples of problems found in a range of physical systems, including preferred models in elementary particle physics. Much of our firm insight to critical phenomena, where the problem is to adequately account for processes in which there is a strong coupling between an infinite number of degrees of freedom, has come from use of a renormalization group method, now a standard method to discuss a multitude of different physical systems. Applied to magnetic systems, the method gives a more complete account of static effects than it does dynamic processes, which are the main subject of the

present discussion. Turning to quasi-periodic systems, the essential features of the fragmented energy spectrum are epitomized in the Hofstadter problem (quantum Hall effect) and arise also in the analysis of lattice vibrations in incommensurate crystal phases and spin excitations in modulated magnets. The appropriate mathematical apparatus, found in the literature on algebraic geometry under spectral properties of periodic difference operators, applies also to the discussion of field-theory models which include a Chern-Simons term, for example.

A second common feature of the two topics chosen for discussion is that, the subtle physical effects are readily accessible to experimental investigation. Indeed, we will make reference to a body of experimental work. Also, at present, neither topic represents a closed book of work, and we aim to identify some of the important outstanding issues.

Two experimental techniques feature prominently in the discussions, namely neutron beam spectroscopy and muon spin relaxation. Neutron spectroscopy is very well established, whereas μ SR is relatively new. In view of the latter situation, we address some comments to the relation between the two techniques.

While our understanding of static critical properties is largely complete the same is not true of dynamic, non-equilibrium critical phenomena. With regard to the first case, the renormalization-group method is a rigorous procedure that lends itself to computation of the exponents and other quantities which characterize static behaviour in the critical region^{1,2}. The concepts of universality classes and relevant and irrelevant variables, and scaling laws which relate various critical exponents are firmly established. However, the method does not conquer all aspects of dynamic critical phenomena. At most, up to now, it has provided asymptotic forms for scaling functions and associated critical exponents³, and a rational basis for dynamic scaling concepts.

In view of this, there is considerable interest in experiments on dynamic spin fluctuations in simple paramagnets. Moreover, these are searching probes of magnetic atomic interactions, as we shall see. Interpretation of the data is a tough challenge to available theoretical methods. Among them there are essentially three types in addition to the renormalization-group. Dynamic scaling provides information, supported by renormalization-group calculations, on the functional behaviour of response functions, but does not in itself provide a means of calculation. The latter can be divided basically in two classes, namely, coupled-mode schemes, and various physically motivated educated guesses consistent with low order frequency sum-rules. By and large, these approximate response functions are not consistent with dynamic scaling. Their main value proves to be in taking account of instrument resolution. Experience has shown that de-convolution of neutron scattering data is tricky, and usually a safer route is to fit data to a parameterized functional form convoluted with the instrument resolution function⁴.

Coupled-mode schemes have the advantage that they provide explicit equations for response functions, which are consistent with dynamic-scaling. There are two basic steps involved in obtaining coupled-mode equations. First, choose an appropriate set of dynamical variables. Here, the starting position is usually the set of conserved variables

that have long lived fluctuations in the critical region, i.e. exhibit critical slowing down. The second step is to make specific approximations to their equations of motion, the upshot of which is a closed set of equations for the response functions of interest. For Heisenberg paramagnets the equations are consistent with the spherical model of static spin correlation functions. Thus, coupled-mode theory can be treated as a complete and consistent description of static and dynamic spin fluctuations.

Several derivations of coupled-mode equations have been presented, each of which provides some insight to the nature of the approximations involved. These are similar to approximations used in the direct-interaction theory of turbulence pioneered by Kraichnan which he quantified by application to a model with an exact solution; full references and a nice review are found in a book by Leslie⁵. Introductions to dynamic critical phenomena, scaling laws and coupled-mode equations are provided by Lovesey⁶.

Applications of coupled-mode theory to the description of wave vector and frequency dependent spin fluctuations in paramagnets, observed by neutron beam techniques, demonstrates that the theory is successful at and above the critical temperature, i.e. it has value outside the critical region. A full set of references, together with a critique of coupled-mode theory, are given by Cuccoli et al.^{7,8}. The aim here is to present an overview of the findings, set against a background of material reviewed by Collins in his book on magnetic fluctuation phenomena⁹, together with links between the interpretation of muon spin relaxation (μ SR) and neutron beam measurements¹⁰.

Turning to the second topic, systems that essentially depend on two or more length scales display various intriguing properties. In condensed matter and materials research, the best known examples of modulated (quasi-periodic) systems are electrons in a crystal subject to an applied magnetic field (Hofstadter problem), incommensurate crystal phases, and magnets with a longitudinally modulated configuration of the moments. Intriguing properties include an energy spectrum that as a function of the ratio of length scales forms a fractal diagram (Hofstadter butterfly). The fragmentation of the energy spectrum is a key element in the integer Quantum Hall Effect; wave functions of states in a gap are localized while those for a band are extended, the localized states being characterized by a Lyapunov exponent. In view of this, the density of states is highly structured. Similar structure appears in response functions which describe scattering experiments and depend on frequency and wave vector transfers.

In confronting predictions for standard models of modulated systems with experimental data there naturally arises a question as to what extent predicted structure might be degraded by collisions, both between excitations and of excitations with impurities and defects. In an incommensurate crystal the latter can be viewed as generating a finite distribution of length scales, and an energy spectrum which is a union of many similar spectra. Hence, singular features in response functions for simple systems might be blurred by collisions, together with some filling of the band gaps. All materials contain impurities and defects to some greater or lesser extent, and thermally activated collisions between excitations are usually present. It is found that a modest value for the

collision damping parameter leads to significant changes in the shape and structure of response functions.

2. Response Functions

Neutron and μ SR experiments on magnetic materials are interpreted in terms of spontaneous fluctuations in the electronic magnetization. The latter is assumed to be proportional to the sum of spin operators $\{S_m\}$ assigned to positions m in a crystal lattice, which contains N unit cells. Wave vectors in Brillouin zone are denoted $\{k\}$ and spatial Fourier components are defined by

$$S(k) = \sum_m e^{-ik \cdot m} S_m . \quad (2.1)$$

A quantity of central interest in the interpretation of experiments is the frequency and wave vector dependent response function,

$$S(k, \omega) = \int_{-\infty}^{\infty} \frac{dt}{2\pi} e^{-i\omega t} \langle S^x(-k) S^x(k, t) \rangle . \quad (2.2)$$

Here, the angular brackets denote a thermal average of the enclosed operators, and $S^x(k, t)$ is the Heisenberg operator obtained from $S^x(k)$. If the Hamiltonian is isotropic, i.e. there are no anisotropy or magnetic field terms defining a preferred axis, the response function (2.2) is independent of the Cartesian label x , as implied by the notation. We use a Bravais lattice, so every atom is a centre of inversion symmetry and $S(k, \omega) = S(-k, \omega)$. Response functions and reciprocal lattices for non-Bravais lattices are discussed in references^{11,12}.

The cross-section for magnetic neutron scattering from an assembly of paramagnetic atoms is proportional to $S(k, \omega)$ ¹². For this experiment ω is the energy transferred to the sample, and the change in wave vector k is measured relative to a Bragg position in reciprocal space.

Relaxation of muon spins due to the fluctuating magnetic environment is expressed in terms of a relaxation rate¹³,

$$\lambda = (\Gamma / N) \sum_k \int_0^{\infty} dt \langle S^x(-k) S^x(k, t) \rangle Y(k) \quad (2.3)$$

where the coupling constant Γ has the dimension of (frequency)², and $Y(k)$ is a structure factor that depends on the location of the positive muon in the crystal lattice¹³. Explicit examples of $Y(k)$ are found in §5.

A theoretical calculation is usually couched in terms of an auxiliary function which is more convenient to work with than $S(\mathbf{k}, \omega)$. For the present purposes we employ a normalized spin-relaxation function $R(\mathbf{k}, t) = R(-\mathbf{k}, t) = R(\mathbf{k}, -t)$ in terms of which^{6,12},

$$S(\mathbf{k}, \omega) = \omega \chi(\mathbf{k}) \left\{ 1 - e^{-\omega/T} \right\}^{-1} \int_{-\infty}^{\infty} \frac{dt}{2\pi} e^{-i\omega t} R(\mathbf{k}, t) = \omega \chi(\mathbf{k}) \left\{ 1 - e^{-\omega/T} \right\}^{-1} F(\mathbf{k}, \omega) , \quad (2.4)$$

where $\chi(\mathbf{k})$ is the isothermal susceptibility, which can be measured by a total scattering experiment, and the second equality defines $F(\mathbf{k}, \omega)$ as the Fourier transform of $R(\mathbf{k}, t)$. In the temperature (T) range of immediate interest it is usually safe to replace the detailed balance factor in (2.4) by (T/ω) . With this approximation $S(\mathbf{k}, \omega)$ is an even function of ω , and the muon relaxation rate,

$$\lambda = (\pi\Gamma / N) \sum_{\mathbf{k}} S(\mathbf{k}, 0) Y(\mathbf{k}) = (\Gamma T / 2N) \sum_{\mathbf{k}} \chi(\mathbf{k}) Y(\mathbf{k}) \int_{-\infty}^{\infty} dt R(\mathbf{k}, t) . \quad (2.5)$$

From (2.4) and (2.5) we see that the interpretation of scattering and muon relaxation experiments entails $\chi(\mathbf{k})$ and $R(\mathbf{k}, t)$. These response functions are discussed in the next section, with particular emphasis on their properties close to and at the critical temperature (T_c).

3. Basic Concepts in Critical Phenomena

Here we discuss critical phenomena in a simple, isotropic Heisenberg magnet. Effects of anisotropy are taken up later in the discussion of μ SR in an antiferromagnetic salt.

In the paramagnetic phase, $T > T_c$, we can appeal to the hydrodynamic equation for the magnetization to obtain the form of $R(\mathbf{k}, t)$ in the limit $ak \ll 1$, where a is the unit cell dimension, and $tT_c \gg 1$. This calculation is based on Onsager's hypothesis that spontaneous fluctuations described by $R(\mathbf{k}, t)$ relax according to the same diffusion equation as do induced non-equilibrium fluctuations. The result is,

$$R(\mathbf{k}, t) = \exp(-k^2 \Lambda |t|) , \quad (3.1)$$

where Λ is the transport coefficient which governs the spin diffusion process. Mode-coupling theory predicts the temperature dependence of Λ to be $\Lambda \sim \kappa^{1/2}$ where κ is the inverse correlation length; the decrease of Λ as $T \rightarrow T_c$ is often referred to a critical slowing down. The response function $F(\mathbf{k}, \omega)$ obtained with (3.1) is a Lorentzian function of ω , centred at $\omega = 0$, with a width $k^2 \Lambda$.

Sufficiently close to T_c the susceptibility is very strongly peaked at $k = 0$ (ferromagnetic fluctuations). For small k ,

$$\chi(k) = \theta / (k^2 + \kappa^2) , \quad (3.2)$$

where θ is mildly temperature dependent, and κ approaches zero at T_c according to a power law,

$$\kappa \sim \left(\frac{T}{T_c} - 1 \right)^{\nu} , \quad (3.3)$$

in which the exponent $\nu = 0.705$ for a three dimensional Heisenberg magnet, for example. Expression (3.2) is the simple Ornstein-Zernike result without modification by Fisher's exponent.

Expressions (3.1) and (3.2) permit λ to be computed in the paramagnetic region, close to T_c . Provided the structure factor $Y(k)$ is finite and well-behaved at the zone centre, it follows from (2.5) that $\lambda \sim (1/\kappa\Lambda)$ and hence λ grows like $(1/\kappa^{3/2})$ as $T \rightarrow T_c$.

For the critical region itself, $k \gg \kappa$, dynamic scaling theory arguments can be employed. The accuracy of the arguments is supported by renormalization-group calculations. Dynamic scaling does not enable $S(k, \omega)$ to be calculated, but just places constraints on its functional form. The theory is not restricted to the critical region. Indeed, concrete information on properties in this region are usually deduced from dynamic scaling by matching with expressions obtained for the hydrodynamic region, $k \ll \kappa$.

For the present discussion, recall that a function of two variables $f(x, y)$ is a homogeneous function of degree z if,

$$f(\mu x, \mu y) = \mu^z f(x, y) , \quad (3.4)$$

for an arbitrary μ . Dynamic scaling theory asserts that the width ω_c of $S(k, \omega)$ is a homogeneous function of the variables κ and k of degree z . The precise definition of $\omega_c(\kappa, k)$ is

$$2 \int_{-\omega_c}^{\omega_c} d\omega F(k, \omega) = 1 . \quad (3.5)$$

Furthermore, there exists a shape function $Z(k/\kappa, x)$ where $x = \omega/\omega_c$ such that,

$$S(k, \omega) = \{T\chi(k)/\omega_c\} Z(k/\kappa, x) . \quad (3.6)$$

This expression together with the properties of the homogeneous functions ω_c and $\chi(k)$ enable us to extract the corresponding temperature dependence of λ .

Inserting (3.6) in (2.5) and converting to a dimensionless integration variable (k/κ) leads to¹³,

$$\lambda \sim \kappa^{1+\eta-z} . \quad (3.7)$$

In arriving at (3.7) use is made of the relation, deduced from (3.4), $\omega_c(\kappa, k) = \kappa^z g(k/\kappa)$, where $g(k/\kappa)$ is a scaling function, and the corresponding relationship for the homogeneous function $\chi(\kappa, k)$, namely,

$$\chi(\kappa, k) \sim \kappa^{-2+\eta} ,$$

where η is Fisher's exponent, and known to be ~ 0.03 for systems of immediate interest. Neglecting η in (3.7), the result is identical with the previous, hydrodynamic, calculation if the exponent $z = 2.5$. The prediction (3.7) holds when the structure factor $Y(\mathbf{k})$ in (2.3) does not influence the divergent behaviour driven by critical fluctuations. This will not be the case with certain high symmetry μ^+ environments for which $Y(\mathbf{k})$ vanishes at the zone centre where critical fluctuations manifest themselves in a simple ferromagnet¹³.

The result $z = 2.5$ also follows directly from the behaviour of ω_c . Using (3.1) to calculate $F(k, \omega)$ in the defining equation for ω_c , (3.5), it is found that $\omega_c = k^2 \Lambda$ in the hydrodynamic region. If $\omega_c(\kappa, k)$ is a homogeneous function of degree z , as asserted, then $\omega_c(\kappa, k) \sim \kappa^{5/2} (k/\kappa)^2$ follows from $\Lambda \sim \kappa^{1/2}$, and thus $z = 2.5$ by definition. This value of z is also obtained from coupled-mode theory evaluated at T_c ¹⁴.

Long range dipolar forces must be included in the interpretation of some experiments, and particularly for the relaxation rate it seems. Dipolar forces violate a number of the simplifying assumptions we have made thus far¹. Spin isotropy is broken, leading to different properties longitudinal and transverse to \mathbf{k} (the longitudinal susceptibility is finite for $k \rightarrow 0$ and $T \rightarrow T_c$) and since the magnetization is no longer a conserved variable relaxational dynamics prevails in the limit of long wavelengths, i.e. a critical exponent $z = 2.0$ is found in the asymptotic limit. In the corresponding analysis of λ there is a cross-over as a function of temperature from $z = 2.5$, obtained for the purely isotropic magnet, to an effective $z = 2.0$ as the critical temperature is approached¹⁵.

4. Coupled-Mode Calculations of $S(k, \omega)$

4.1 Analytic Results

The coupled-mode equation for a purely isotropic Heisenberg paramagnet has the form of a single integro-differential equation for $R(k, t)$ ⁶. Other quantities that occur in the equation are the exchange interaction and wave vector-dependent isothermal susceptibility, and implicitly the crystal lattice. It can be shown that the equation is consistent with the spherical model approximation for the susceptibility. When this form is adopted the coupled-mode theory becomes a self-contained theory for $R(k, t)$, given the exchange of interactions and lattice type. The spirit of the coupled-mode theory for critical phenomena is summarized by Stanley¹⁸ in the context of the liquid-gas phase transition. It might be enlightening to compare and contrast his summary with the reasoning employed in⁶ to derive the coupled-mode equation for a paramagnet.

In the limit of small wave vectors it is possible to show analytically that the coupled-mode equation for a ferromagnet predicts:

- (a) the spin diffusion constant for $T > T_c$ is proportional to $\kappa^{1/2}$ ⁶.
- (b) with $T = T_c$ and $k \rightarrow 0$ the half width at half height for $F(k, \omega)$, plotted as a function of ω for fixed k , is proportional to $k^{5/2}$ ¹⁴.

and

- (c) $R(k, t)$ at T_c is almost a Gaussian function of t for small t , by which we mean $\omega_0 t \ll 1$ where ω_0^2 is the second normalized frequency moment of $F(k, \omega)$ ¹⁶.

Results (a) and (b) are consistent with dynamic scaling and renormalization-group calculations. Experimental data which supports the predicted critical slowing down is reviewed by Collins⁹ and Hohenemser et al.¹⁰.

A $k^{5/2}$ dependence at T_c of the half width has been demonstrated very convincingly for EuO. The available data spans two decades in k and five decades in the magnitude of the half width¹⁰. Other data is reviewed by Collins⁹.

Data for $R(k, t)$ at small wave vectors and $T = T_c$, obtained by the spin echo technique for EuO, is not consistent with the almost Gaussian time dependence predicted by coupled-mode theory (c), although observed values of the line width, ω_c , are in excellent accord with a $k^{5/2}$ dependence ($z = 2.5$) and magnitudes extrapolated from conventional neutron experiments at larger values of k . These findings have been reconciled with theory through the introduction of dipolar forces in the Hamiltonian. It has been established that the modified coupled-mode theory predicts cross-over in the width and line-shape at distinctly different values of k . Cross-over to $z = 2.0$ occurs at a k value which is about an order of magnitude smaller than the value for cross-over in static properties and the line-shape¹⁷, i.e. the spin echo experiments are not made with a k small enough to observe $z = 2.0$ in the width although the line-shape has crossed over to an

exponential form. We can conclude that the restriction placed on $R(k,t)$ by dynamic scaling is a subtle issue, since both isotropic and dipolar Hamiltonians lead to $z = 2.5$, within the coupled-mode theory, until an extreme value of k is achieved.

The neutron scattering technique enables $F(k,\omega)$ to be measured throughout the Brillouin zone. To interpret such data it is necessary to use numerical techniques to solve the coupled-mode equation for $R(k,t)$ and then form $F(k,\omega)$; a method is described by Cuccoli et al.⁷. The following sub-section is devoted to a brief survey of the findings to date.

4.2 Numerical and Experimental Results

The relaxation function has been calculated for realistic models of EuO, EuS and Pd₂MnSn and compared results with neutron scattering data^{7,8}. These three ferromagnetic materials share the same magnetic structure, namely f.c.c. The Heusler compound Pd₂MnSn is metallic, and an analysis of the measured spin wave spectrum reveals that a Heisenberg model with an extended exchange interaction, out to eight co-ordination shells, furnishes an adequate description. A corresponding analysis of the insulating europium compounds reveals that the dominant exchange interactions are nearest and next-nearest neighbour, i.e. two exchange parameters suffice. For EuO these have the same (ferromagnetic) sign, whereas in EuS they have opposite signs and the nearest-neighbour ferromagnetic exchange dominates. Hence, for all materials there are values of the exchange parameters derived from separate experiments.

Using these parameters and an f.c.c. lattice, one obtains tolerable agreement between the calculated $F(k,\omega)$ and neutron scattering data. For EuO data are available for $T = T_c$ and $1.68T_c$ and $2.0 T_c$, over a wide range of wave vectors. In comparing theory and experimental data it is important to allow for the resolution of the neutron spectrometer; for small k ($=0.4 \text{ \AA}^{-1}$) it is essential in order to have a meaningful result. At $T = T_c$ and the largest wave vector $k = 1.0 \text{ \AA}^{-1}$ the experimental $F(k,\omega)$ is squarer in shape than our calculated function, but the data does not support the concept of a collective mode. We will return to this topic.

Data for EuS at $1.51T_c$ and $3.0T_c$ contains larger scatter than that in the data we have for EuO. Bearing this in mind, the agreement between theory and experiment is judged to be satisfactory. For k at the zone boundary along the (1,0,0) direction, the calculated $F(k,\omega)$ is quite square in shape, but as in the case of EuO we do not believe there is real evidence in favour of a collective mode.

At $T = T_c$ and for small k there is next to no difference in $F(k,\omega)$ calculated for the models of EuO and EuS. But there are striking differences for large wave vectors. A strong dependence of $F(k,\omega)$ for EuS on the direction of k , a consequence of the competing nature of the exchange parameters, is absent in EuO. This prediction has not been the subject of experimental investigation.

The importance of the lattice type has been established. For example, a calculation with EuO parameters performed for a s.c. lattice is significantly different from the calculation for an f.c.c. lattice and the experimental data.

We turn now to an interpretation of data for Pd_2MnSn ⁸. The experiment was performed with a sample temperature of $1.1T_c$ and three wave vectors in the (1,1,1) direction. Particularly good agreement is obtained between the calculated spectrum and data for $k = 0.5k_{ZB}$, and $0.7 k_{ZB}$, and it is tolerable for $k = 0.92 k_{ZB}$. A squaring of the spectrum is obtained for the largest wave vector. In the experimental data, this effect is more evident in EuS than in EuO and Pd_2MnSn , but even in EuS it is not a striking feature.

Next we comment on calculations performed for a model of Fe, a metallic b.c.c. ferromagnet⁸. There has been debate in the literature as to whether it is physically meaningful to use a Heisenberg exchange model to interpret data on Fe. We believe that it is hasty reasoning to discard this approach on the basis of currently available data. The calculations, using various sets of exchange parameters, are the most sophisticated and extensive calculations reported to date, and afford the possibility of a stringent test of the model. Looking at available data the results appear to be tolerable, but a more precise statement must await the outcome of further experiments.

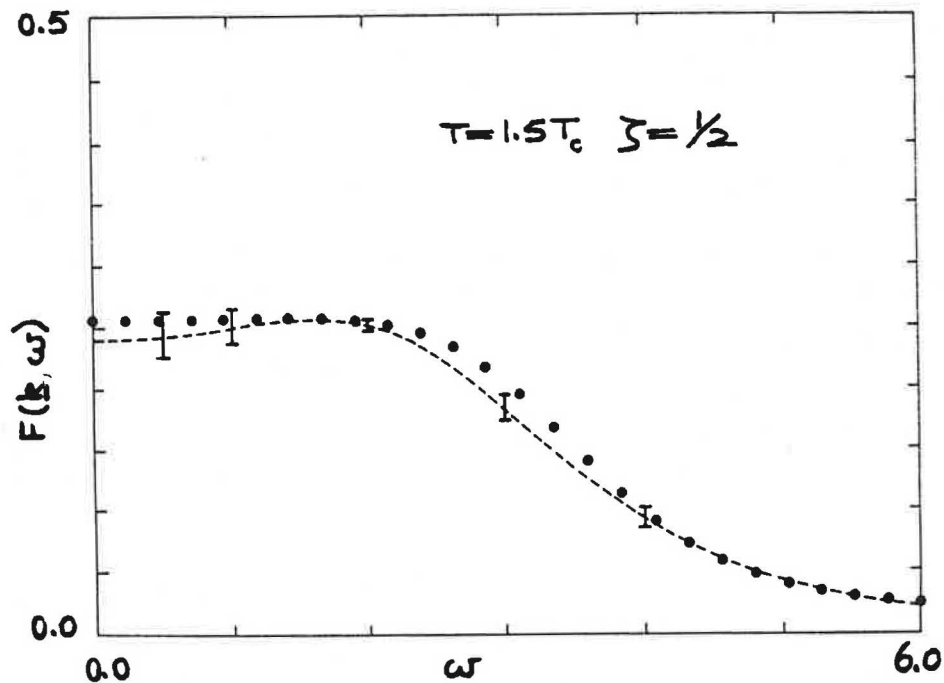


Fig. (1) Experimental and theoretical results for $F(k, \omega)$ are displayed for gadolinium at $T = 1.5T_c$ with $k = 4\pi (\frac{1}{2}, \frac{1}{2}, 0)/a$, and ω in TH_z . In calculating $F(k, \omega)$ the input data is the lattice type (h.c.p.), $J = 0.543$ meV, $T_c = 300\text{K}$ and $S = 7.63/2$. The experimental results are generated from a damped harmonic oscillator form for $F(k, \omega)$ with parameters given by Cable and Nicklow (1989)⁴. The indicated spread in the data is a conservative estimate provided by Dr Cable (private communication). Results from ref¹⁹.

Fig. (1) illustrates the relaxation function for gadolinium at $1.5T_c$. In this instance, a comparison of experimental data and theoretical calculations demonstrate that the

exchange interaction at $1.5T_c$ is significantly different from the interaction deduced from the analysis of spin wave dispersion data¹⁹. Another notable feature of this work is the indication of a collective mode excitation in the weak peak at $\omega \sim 2.0 TH_z$. To date, the experimental data for gadolinium is the clearest evidence for such a feature, albeit very heavily damped. It remains to be seen if coupled-mode theory with a single exchange parameter, as used in Fig. (1), provides a good account of available neutron data at T_c , and muon spin relaxation data²⁵.

5. Muon Spin Relaxation: Antiferromagnetic Exchange

The technique of muon (μ^+) spin relaxation applied to magnetic materials possesses several attractive features²⁰. Perhaps none more so than the ability to make measurements without use of an applied magnetic field, since it gives μ SR a striking advantage over most other techniques used to study paramagnetic and critical spin fluctuations. Set against this, the μ SR relaxation rate, λ , is a bulk response function, unlike the neutron scattering cross-section, that does not display distinct signatures of spin-wave and paramagnetic collective excitations. Also, the site of the implanted muon must be determined, and if it is not a completely passive probe, e.g. μ^+ is chemically active, interpretation of relaxation rates may be far from straightforward in terms of magnetic properties of the target material. In the following discussion of μ SR in antiferromagnetic salts we assume for the implanted muon a unique site (zero-point motion is neglected) and that it is a completely passive observer of spin fluctuations.

From the theory of relaxation in ferromagnets we deduce that in the ordered state λ is dominated by fluctuations in the component of magnetization parallel to the easy axis¹³. For uniaxial magnets the same situation prevails in the critical and paramagnetic ($T \geq T_c$) states. In an antiferromagnetic salt, described by a Heisenberg model, the order parameter (staggered magnetization) is not a conserved variable, in contrast to an isotropic ferromagnet discussed in previous sections. Furthermore, in a temperature region close to T_c axial anisotropy plays an essential role, and it renders mode couplings ineffective, for both ferro and antiferromagnetically coupled magnets²¹. In consequence, the conventional theory of spin fluctuations is adequate and the relaxation rate, Γ , associated with the order parameter (staggered magnetization) is proportional to κ_z^2 , where $\kappa_z (= 0, T = T_c)$ is the inverse correlation length for fluctuations parallel to the easy (z) axis. At a sufficiently high temperature the magnet is effectively isotropic in nature; mode couplings are then operative and change the temperature dependence of the order parameter relaxation rate to $\kappa^{3/2}$ (the corresponding result for a ferromagnet is $\kappa^{5/2}$). We will use these results to predict the relaxation rate of muon signals in antiferromagnetic salts, and illustrate our findings by application to materials with the rutile structure, e.g. MnF_2 , FeF_2 .

Relaxation of the muon signal occurs largely because of spin-flip processes generated by fluctuations in the isotropic (hyperfine) and dipolar magnetic fields experienced by the implanted muons. In calculating the relaxation rate, λ , we single out (electronic) spin fluctuations in the direction of the easy (z) axis because uniaxial magnetic anisotropy suppresses fluctuations in other components²².

Consider first the isotropic mechanism for relaxation, described by the Hamiltonian

$$\sum_{\ell} A_{\ell} \mathbf{I} \cdot \mathbf{S}(\ell) = \sum_{\alpha, \ell} A_{\ell} I^{\alpha} S^{\alpha}(\ell) , \quad (5.1)$$

where \mathbf{I} and \mathbf{S} are spin operators associated with the muon and electronic magnetic moments, respectively, and the sum extends over all ions for which the coupling constant A_{ℓ} is significant. If the initial and final muon spin states are $|I, m\rangle, |I, m'\rangle$ the relaxation rate created by the hyperfine mechanism, obtained from Fermi's Golden Rule, is

$$\lambda_h = \frac{(2/\hbar^2)}{|\langle m|I^{\alpha}|m'\rangle|^2} \sum_{\alpha} |\langle m|I^{\alpha}|m'\rangle|^2 \sum_{\ell, \ell'} A_{\ell} A_{\ell'} \int_{-\infty}^{\infty} dt \langle S^{\alpha}(\ell, t) S^{\alpha}(\ell', 0) \rangle . \quad (5.2)$$

In deriving this expression for λ_h we have used $\langle S^{\alpha} S^{\beta} \rangle = 0$ for $\alpha \neq \beta$; this identity is not valid if the Heisenberg model contains interactions which break conservation of the total z-component of the magnetization, e.g. dipolar forces. For a uniaxial magnet it is this component of the magnetization that witnesses critical fluctuations. Thus, since $m \neq m'$ in (5.2) we conclude that the hyperfine relaxation rate is not enhanced by critical fluctuations in a uniaxial magnet. In the limit of an *isotropic* magnet (5.2) reduce to,

$$\begin{aligned} \lambda_h &= (1/\hbar^2) \sum_{\ell, \ell'} A_{\ell} A_{\ell'} \int_{-\infty}^{\infty} dt \langle S^{\alpha}(\ell, t) S^{\alpha}(\ell', 0) \rangle \\ &= (2\pi/\hbar N) \sum_{\ell, \ell'} A_{\ell} A_{\ell'} \sum_{\mathbf{k}} \cos[\mathbf{k} \cdot (\ell - \ell')] S(\mathbf{k}, 0) \\ &= (2T/\hbar^2 N) \sum_{\ell, \ell'} A_{\ell} A_{\ell'} \sum_{\mathbf{k}} \cos[\mathbf{k} \cdot (\ell - \ell')] \{ \chi(\mathbf{k}) / \tilde{K}(\mathbf{k}, 0) \} . \end{aligned} \quad (5.3)$$

Here, we have used the standard definition of the van Hove response function $S(\mathbf{k}, \omega)$, observed in neutron beam experiments, and its relation to the isothermal susceptibility, $\chi(\mathbf{k})$, and Laplace transform of the memory function, $\tilde{K}(\mathbf{k}, s)$. The latter can be regarded as a collisional self-energy, while $\tilde{K}(\mathbf{k}, 0) = \Gamma(\mathbf{k})$ is the relaxation rate for the magnetization mentioned in the introductory material⁶.

Turning to relaxation generated by fluctuations in the dipolar field experienced by a muon, we use an expression for λ_d derived by Lovesey et al. (1992)¹³. If ℓ, ℓ' label magnetic ions equidistant from a muon, and there is a random distribution of domains in the sample, so it is appropriate to average over orientations of the easy (z) axes,

$$\begin{aligned} \lambda_d &= \left(\frac{\pi\gamma}{10}\right) \sum_{\ell, \ell'} \sum_Q (4-Q^2) Y_Q^2(\ell) Y_Q^{*2}(\ell') \int_{-\infty}^{\infty} dt \langle S^z(\ell, t) S^z(\ell', 0) \rangle \\ &= \left(\frac{\pi\gamma}{5N}\right) \sum_{\ell, \ell'} \sum_Q (4-Q^2) Y_Q^2(\ell) Y_Q^{*2}(\ell') \sum_k \cos[\mathbf{k} \cdot (\ell - \ell')] \{ \chi_z(\mathbf{k}) / \Gamma_z(\mathbf{k}) \}. \end{aligned} \quad (5.4)$$

Here, $Y_Q^2(\ell)$ is a spherical harmonic of order 2 and rank Q ($=0, \pm 1$) and the coupling constant,

$$\gamma = \frac{8}{3} (g\mu_B \mu_N / \hbar d^3)^2, \quad (5.5)$$

where g is the gyromagnetic factor for the ions at a distance d from the muon. The expression (5.4) applies to a uniaxial magnet; in the isotropic limit all components of the magnetization are enhanced by critical fluctuations so an additional factor 3 should be introduced.

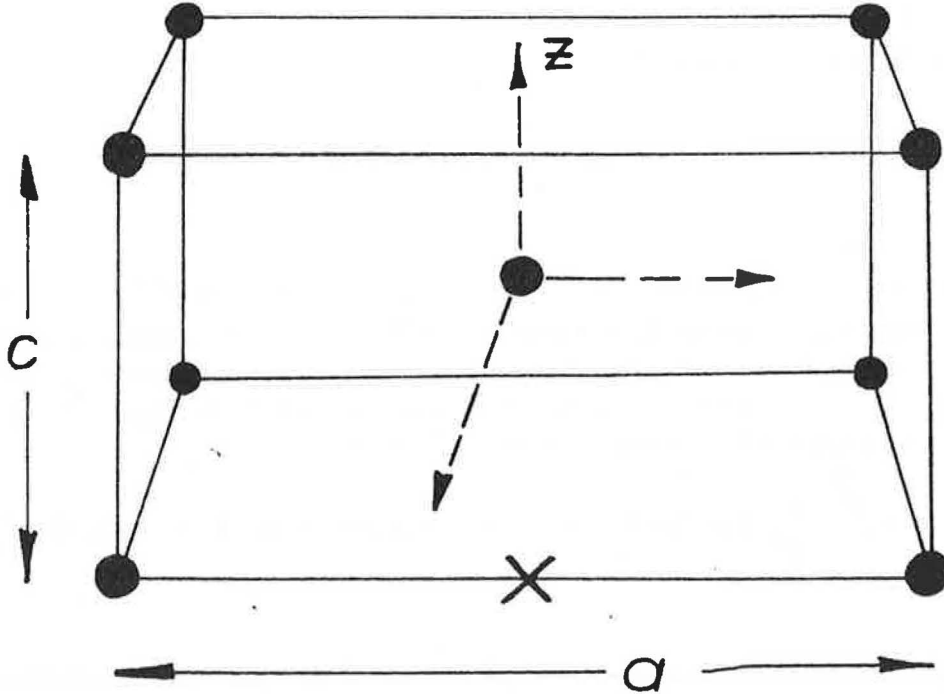


Fig. 2. The magnetic unit cell of the rutile salts MnF_2 and FeF_2 is illustrated together with the octahedral site (x) for an implanted muon (de Renzi et.al. 1984)²³. In calculating the fluctuating dipole field a total of six ions are included, two at a distance $(a/2)$ and four at a distance $(a/2)(1+f^2)^{1/2}$ where $f = (c/a)$; the two sets of ions belong to different sublattices.

Let us now consider the implications for μSR experiments on antiferromagnets with a rutile structure. Experimental work²³ indicates that implanted muons occupy sites with an octahedral symmetry, illustrated in Fig (2). If the magnet is isotropic in spin space, and the hyperfine interaction is dominated by the nearest-neighbour pair of ions,

$$\lambda_h = \left(\frac{4TA^2}{\hbar^2 N} \right) \sum_k \{1 + \cos(ak_x)\} \{\chi(k)/\Gamma(k)\} \\ \equiv 0.11 (T_c A^2 v_o^{1/3} \chi_o / \hbar Q \kappa^{1/2}) ; T \rightarrow T_c , \quad (5.6)$$

where χ_o is the susceptibility at T_c , v_o is the volume per spin, and Q is the non-universal material constant,

$$Q^2 = v_o T_c / \chi_o (2\pi)^3 . \quad (5.7)$$

In arriving at the estimate in (5.6), the geometric factor has been evaluated for $k = w = (2\pi/a) (1, 1, f)$ at which the staggered susceptibility

$$\chi(k) = \chi_o / \left\{ v_o^{2/3} (\kappa^2 + |k-w|^2) \right\} , \quad (5.8)$$

achieves the maximum value. The result,

$$\hbar\Gamma(k) = 8.4 Q \kappa^{3/2} , T \rightarrow T_c , \quad (5.9)$$

used in (5.6) was obtained from a mode-coupling calculation²¹. In deriving the corresponding expression for λ_d the first two shells of ions surrounding an octahedral site have been used on the grounds that more distant shells give a negligible contribution, e.g. MnF_2 , $f = (c/a) = 0.680$ and values of d^6 for the first three shells are in the ratio, 1:0.32:0.04. Using (5.4), extended to two shells of ions,

$$\lambda_d = \left(\frac{\gamma T}{2N} \right) \sum_k \{ \chi(k)/\Gamma(k) \} \left\{ 1 + r + s \cos(ck_z) + \cos(ak_x) [1 + s + r \cos(ck_z)] \right\} , \quad (5.10)$$

in which

$$\left. \begin{matrix} r \\ s \end{matrix} \right\} = \frac{2}{(1+f^2)^5} \left[(2f^2 - 1)^2 \pm 9f^2 \right] .$$

Evaluating the geometric factor in (5.10) for $k=w$, leads with the introduction of a factor 3 to the result,

$$\lambda_d \cong 0.04 \left(\frac{\hbar \gamma T_c \chi_o \nu_o^{1/3}}{Q \kappa^{1/2}} \right) \left\{ 1 + \frac{4(2f^2-1)^2}{(1+f^2)^5} \right\}, \quad (5.11)$$

where γ is obtained from (5.5) with $d = (a/2)$. The estimates predict that relaxation rates for isotropic antiferromagnets diverge as $T \rightarrow T_c$ with a power-law dependence $(1/\kappa)^{1/2}$.

In a *uniaxial* magnet the inverse correlation length associated with fluctuations in the plane perpendicular to the easy axis saturates as $T \rightarrow T_c$ to a finite value κ_o . At sufficiently high temperatures, $\kappa_z \gg \kappa_o$ and the estimates for the relaxation rates are appropriate. But very close to T_c , $\kappa_z \ll \kappa_o$ and the anisotropy energy changes the nature of the critical fluctuations manifest in the component of the staggered magnetization parallel to the easy axis. It is useful to consider a cross-over temperature T_o at which $\kappa_o = \kappa_z$, e.g. MnF_2 , $\kappa_o = 0.054 \pm 0.01 \text{ \AA}^{-1}$, $T_c = 6.7.5\text{K}$, $Q = 2.2 \pm 0.1 \text{ meV \AA}^{3/2}$ and $T_o = 1.034 T_c = 70\text{K}^{21,24}$. For anisotropic magnets ($T < T_o$) the critical state is characterized by two competing length scales. The isotropic scaling concept is extended so that the relaxation rate Γ depends homogeneously on the anisotropy parameter κ_o in the limit that this parameter is small²¹,

$$\hbar \Gamma(k) = Q \kappa_o^{3/2} R(k/\kappa_o, \kappa_z/\kappa_o), \quad (5.12)$$

where the scaling function $R(x,y)$ is universal in the sense that it does not depend on material parameters, but rather on the basic symmetry and conservation-law properties of the magnet. In the extreme anisotropic limit, $\kappa_z \sim 0$,

$$\hbar \Gamma(k) \rightarrow Q \kappa_o^{3/2} (k/\kappa_o)^2 \zeta, \quad (5.13)$$

where ζ is a dimensionless constant that might be derived from a particular theory, e.g. mode-coupling or renormalization group calculations. If we employ (5.13) to estimate λ_d , following the steps that led to (5.11),

$$\lambda_d \cong 0.08 \left(\frac{\hbar \gamma T_c \chi_o \nu_o^{1/3} \kappa_o^{1/2}}{Q \zeta \kappa_z} \right) \left\{ 1 + \frac{4(2f^2-1)^2}{(1+f^2)^5} \right\}. \quad (5.14)$$

Hence, in the extreme anisotropic limit λ_d increases (as $T \rightarrow T_c$) with a power-law dependence $(1/\kappa)$ whereas, as noted earlier, λ_{\parallel} is not affected by critical fluctuations.

Several aspects of the estimates merit comment. First, the geometric factors in the integrands of the k -integrations in the expressions (5.3) and (5.4) for λ_h and λ_d do not directly influence properties of the relaxation rates, in contrast to situations that can arise with ferromagnetic materials¹³. The origin of the strong influence of geometric factors in ferromagnets is the coincidence of chemical and magnetic order. For antiferromagnetic materials critical fluctuations arise in the vicinity of a magnetic superlattice Bragg reflection $k = \omega$. Another aspect is that the temperature dependence of λ predicted for isotropic and uniaxial antiferromagnets is precisely the same as that for the NMR linewidth ($1/T_2$). Finally, we note that using (5.14) and parameters for MnF_2 ,

$$\lambda_d \equiv (\kappa_o / \kappa_z) (0.012 / \zeta) \mu s^{-1} ,$$

and $(\kappa_o / \kappa_z) \sim 11$ for a temperature 0.06% above T_c and $\kappa_z \propto (T - T_c)^\nu$ with $\nu \sim 2/3$. If $\zeta \sim 1$ the prediction for λ_d is well within the range accessible in experiments. Parameters for FeF_2 and MnF_2 are very similar apart from κ_o which is a factor 2.7 larger in the first salt, i.e. FeF_2 is more anisotropic than MnF_2 .

6. Quasi-Periodic Magnets

There is a variety of physical systems whose properties crucially depend on the interplay of two, or more, different length scales. When one scale is set by a lattice unit cell dimension, the second scale can usefully be regarded as imposing a modulation which, in general, is incommensurate with the lattice. The modulation can be created by atomic forces or an applied perturbation. Examples of the first type of system are ordered magnetic materials in which inter-atomic interactions create a modulated magnetization, and materials where anharmonic forces lead to an incommensurate lattice phase. A much studied case of a modulated system created by an applied perturbation is the dynamics of electrons in a crystal subject to a magnetic field, for which the inverse of the field strength is the second length scale. The effect of the modulation on the dynamic properties, observed in appropriate response functions, is dramatic. For example, a simple ferromagnet contains spin waves whose energy is strongly dispersive. It is shown that even a long range longitudinal modulation of the magnetization removes all vestige of the spin wave excitation and the new energy spectrum is essentially dispersionless; some features are illustrated in Fig. (3).

The energy spectrum, or band structure, of a modulated system is a celebrated example of a fractal diagram. Its key features were recognized and explored by Hofstadter²⁶ in his study of electron motion in a crystal subject to a magnetic field. Energy bands plotted for different fields generate a striking diagram which Hofstadter likened to a butterfly, and the term butterfly diagram has become firmly established.

His work is a masterful example of numerical analysis. So much so, perhaps, that subsequent studies of models of modulated systems mostly exploit numerical methods of the same or similar type. Another factor contributing to the dominance of numerical

methods is that the Hamiltonian which describes the most basic standard models is a tridiagonal matrix for which there are efficient and accurate diagonalization algorithms. While the existence of these algorithms means that the calculation of response functions, the most fundamental of which is the density of states, is not an awesome task today it is nonetheless a non-trivial undertaking. Clearly there is both room and a need for purely analytic methods of calculation.

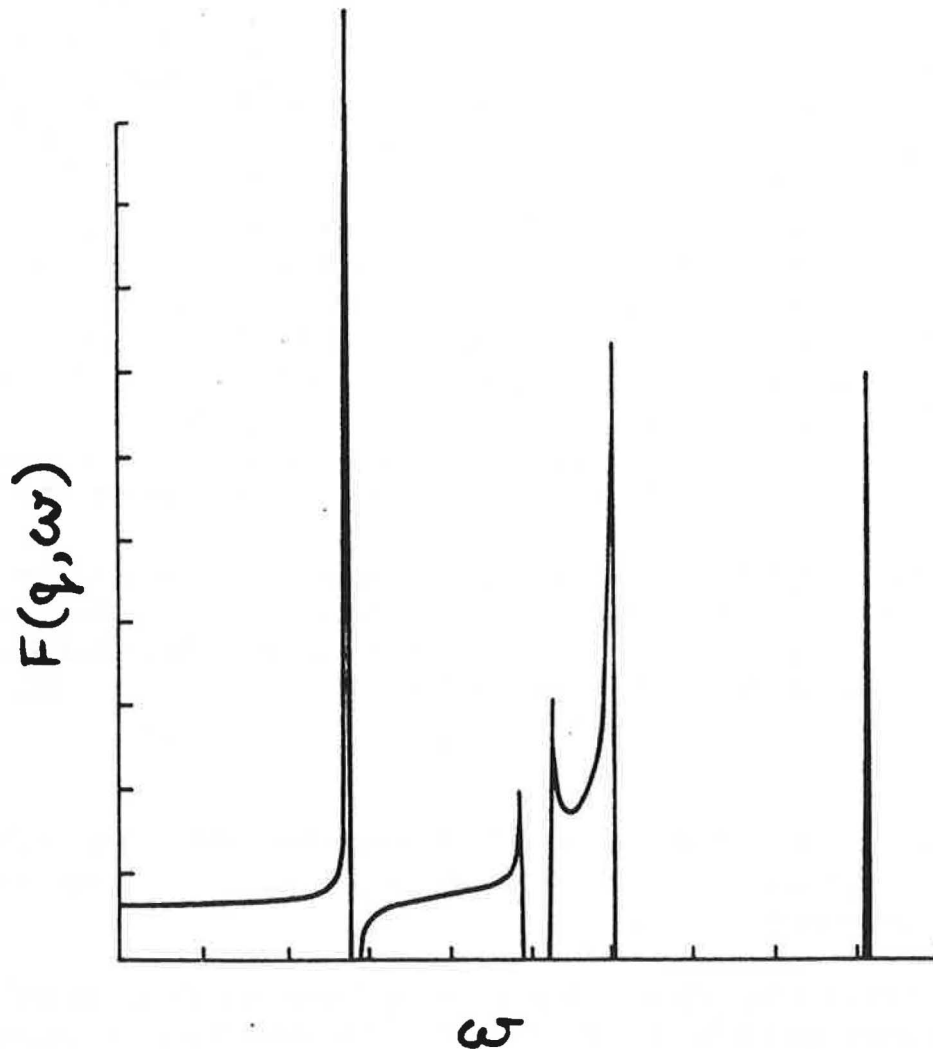


Fig. 3. The response function for transverse spin fluctuations in a longitudinally modulated magnet, in arbitrary units, for a periodicity $N = 8$. Referring to eqn (7.9), the displayed quantity is proportional to $\{-Im. G(\omega)/\omega\}$, as in (8.6). Parameters in W_n defined in equ. (7.1) are $\beta = 0.141$ and $\alpha = -4\beta \cos(\pi/4)$ and $q = (2\pi/5)$.

Here we describe an algebraic method to calculate dynamic response functions and illustrate it by application to some models of modulated systems²⁷. Success in constructing the method hinges on two features of the models. First, although physical systems of interest are three-dimensional, the standard models reduce to a one-dimensional

eigenvalue equation. Response functions are conveniently obtained from an appropriate Green function, or propagator, and the equation of motion is actually an inhomogeneous second-order difference equation. The second important feature is approximation of the modulation by a rational value, as in all numerical studies, so the coefficients in the difference equation are periodic. A truly incommensurate case might be approached by using a suitable sequence of rationals, such as the Fibonacci sequence. However, the precise form of the spectrum for an irrational modulation is likely to be merely a mathematical curiosity, for the degree of fragmentation in the (bounded) spectrum is proportional to the size of the denominator (N) in the rational fraction. In consequence, use of progressively higher-order rationals to approach an irrational generates a level of fine structure which eventually is not resolvable in experiments, either in the laboratory or on a computer.

Features of the physical models have much in common with some topics of current interest in mathematics, and pursuits in algebraic geometry in particular. In this respect, we are thinking mainly of work on the spectrum of periodic difference operators and associated algebraic curves. The algebraic curves, and their orthogonal meromorphic functions and the holomorphic differential form, studied by van Moerbeke and Mumford²⁸, have a physical realization in models of modulated systems. There is the possibility that yet further insight to the structure of dynamic response functions may come from the minds of researchers fluent in branches of mathematics mentioned.

For a longitudinally modulated magnet, of the type discussed here, the magnetic moments order in the z -direction, say, and have a magnitude which varies with distance along this axis. In the simplest case, the moments are described by a single wave vector $Q = (0, 0, Q)$ such that the spin moment at site ℓ is,

$$\langle S_{\ell}^z \rangle \propto \cos(zQ) .$$

Such a configuration has been observed at low temperatures²⁹ in the compound PrNi_2Si_2 , although it was first observed in rare earth metals; neutron scattering data and a set of useful references are provided in^{30,32}.

A theory for the response function of a standard model of a modulated system is briefly surveyed in the following section. A minimum of detail is given since the theory has recently been reviewed²⁷.

7. Analytic Expression for the Response Function of a Quasi-Periodic Magnet

In the absence of the longitudinal modulation of the configuration of magnetic moments, the transverse spin fluctuation spectrum is exhausted by spin wave excitations which are strongly dispersive⁶. Even a very long range modulation of the magnetic moments removes the strong dispersion, and produces a finite intensity at zero frequency and a singular, fragmented structure at finite frequencies.

eigenvalue equation. Response functions are conveniently obtained from an appropriate Green function, or propagator, and the equation of motion is actually an inhomogeneous second-order difference equation. The second important feature is approximation of the modulation by a rational value, as in all numerical studies, so the coefficients in the difference equation are periodic. A truly incommensurate case might be approached by using a suitable sequence of rationals, such as the Fibonacci sequence. However, the precise form of the spectrum for an irrational modulation is likely to be merely a mathematical curiosity, for the degree of fragmentation in the (bounded) spectrum is proportional to the size of the denominator (N) in the rational fraction. In consequence, use of progressively higher-order rationals to approach an irrational generates a level of fine structure which eventually is not resolvable in experiments, either in the laboratory or on a computer.

Features of the physical models have much in common with some topics of current interest in mathematics, and pursuits in algebraic geometry in particular. In this respect, we are thinking mainly of work on the spectrum of periodic difference operators and associated algebraic curves. The algebraic curves, and their orthogonal meromorphic functions and the holomorphic differential form, studied by van Moerbeke and Mumford²⁸, have a physical realization in models of modulated systems. There is the possibility that yet further insight to the structure of dynamic response functions may come from the minds of researchers fluent in branches of mathematics mentioned.

For a longitudinally modulated magnet, of the type discussed here, the magnetic moments order in the z -direction, say, and have a magnitude which varies with distance along this axis. In the simplest case, the moments are described by a single wave vector $Q = (0, 0, Q)$ such that the spin moment at site l is,

$$\langle S_l^z \rangle \propto \cos(zQ) .$$

Such a configuration has been observed at low temperatures²⁹ in the compound PrNi_2Si_2 , although it was first observed in rare earth metals; neutron scattering data and a set of useful references are provided in^{30,32}.

A theory for the response function of a standard model of a modulated system is briefly surveyed in the following section. A minimum of detail is given since the theory has recently been reviewed²⁷.

7. Analytic Expression for the Response Function of a Quasi-Periodic Magnet

In the absence of the longitudinal modulation of the configuration of magnetic moments, the transverse spin fluctuation spectrum is exhausted by spin wave excitations which are strongly dispersive⁶. Even a very long range modulation of the magnetic moments removes the strong dispersion, and produces a finite intensity at zero frequency and a singular, fragmented structure at finite frequencies.

When the external wave vector q is parallel to the modulation wave vector Q , the equation of motion for spin-flip operators reduces to a second-order difference equation with coefficients (n an integer)

$$W_n = 1 + \alpha \cos(q+nQ) + \beta \cos 2(q+nQ) , \quad (7.1)$$

in which the energy parameters α, β are related through

$$\alpha / \beta = -4 \cos Q . \quad (7.2)$$

The response function is obtained from a propagator, or Green function, expressed in terms of two infinite continued fractions in which the coefficients are,

$$t_n^2 = W_n W_{n+1} . \quad (7.3)$$

Manipulation of the continued fractions is made easier by expressing them in terms of two sets of polynomials (in the frequency ω) derived from the common recursion relation,

$$R_n = \omega R_{n-1} - t_{n-1}^2 R_{n-2} . \quad (7.4)$$

The two sets of polynomials $\{A_n\}, \{B_n\}$ are distinguished by their initial values, namely,

$$A_{-1} = B_0 = 1, \text{ and } A_0 = B_{-1} = 0 . \quad (7.5)$$

At this juncture it might be observed that the problem defined is very amenable to numerical methods. Efficient algorithms exist for the diagonalization of tri-diagonal matrices, or the straightforward calculation of $\{A_n\}, \{B_n\}$ from (7.4). Such a method inevitably means that results are for a rational value of Q , and presumably approximate closely to those for an irrational (incommensurate) value. This is confirmed in calculations made with numbers from a Fibonacci sequence which converge to an irrational. Use of successively higher order rational approximates generate increasingly fine structure in the response function. Hence, beyond a certain point the additional structure is possibly of only mathematical interest, since it is not likely to be resolved in an experiment. Hofstadter's viewpoint was that common sense tells that there can be no physical effect stemming from the irrationality of some parameter²⁶.

A numerical method is tantamount to using

$$Q = 2\pi M / N \quad (7.6)$$

where M and N are (coprime) integers. With this representation for the modulation wave vector t_n is N -fold periodic, i.e. $t_n = t_{n+N}$. In consequence, the continued fractions required for the propagator are fixed points of a fractional linear transformation, and the propagator can be expressed in closed analytic form. Note that the algebraic method referred to makes no use of translational invariance of the lattice on which the magnetic atoms are arranged, for this invariance is not present in the incommensurate magnet that is being modelled. Use of translational invariance and the representation (7.6) for Q leads to a response function which is zero everywhere except at the N normal mode frequencies.

The propagator which describes transverse spin fluctuations in a modulated magnet is conveniently expressed in terms of the function,

$$L_N(\omega) = (2\Omega_N)^2 - (A_{N-1}(\omega) + B_N(\omega))^2, \quad (7.7)$$

where

$$\Omega_N = t_0 t_1 \dots t_{N-1}, \quad N \geq 2. \quad (7.8)$$

If we denote the propagator by $G(\omega)$ then the response function observed in an experiment is,

$$Im. G(\omega) = \begin{cases} 0 & ; L_N(\omega) \leq 0 \\ (-\omega\chi/2) |B_{N-1}(\omega)| \{L_N(\omega)\}^{-1/2} & ; L_N(\omega) > 0 \end{cases} \quad (7.9)$$

In this expression, $\chi = 2S/W_0$ is the wave vector dependent susceptibility (S is the magnitude of the spin moment) and the imaginary part of G is calculated with the rule $\omega \rightarrow \omega + i\eta$ and $\eta \rightarrow 0^+$.

$L_N(\omega)$ is a polynomial in ω of degree $2N$ and $L_N(\omega) = 0$ has only real roots. A band (gap) is defined by $L_N(\omega) > 0$ (≤ 0). For N even (odd) there are $N-1$ (N) bands, and $B_{N-1}(\omega)$ is of one sign in a band. Additional properties of the spectrum together with several specific examples of $Im. G(\omega)$ can be found in papers by Lovesey²⁷ and Lantwin³¹. It is usually the case that $Im. G(\omega)$ is singular at the band edges; such behaviour is difficult to extract from numerical work, and indeed the existence of the singularities makes the correct calculation of $Im. G(\omega)$ quite a subtle numerical problem. Examples of the spectrum of spin fluctuations in undamped modulated magnets are provided in Figs (3,4).

8. Examples of the Response Function Including the Influence of Collision Damping

It is entirely possible to convincingly analyse some specific models of collision damping, such as that generated by substitutional defects. Damping due to collisions between excitations is usually a more demanding theoretical task. An alternative

viewpoint is to introduce into the theory a phenomenological damping parameter (γ) and model collisional effects by complexification $\omega \rightarrow \omega + i\gamma$ of the exact analytic expressions provided in §7. Such a scheme is justified when there is no experimental evidence to favour a specific mechanism. In the present case, of fluctuations in modulated (quasi-periodic) system, it is a sensible method by which to gauge effects of collision damping in models of observed response functions. It will be shown that our treatment of damping predicts non-trivial changes in the spectra.

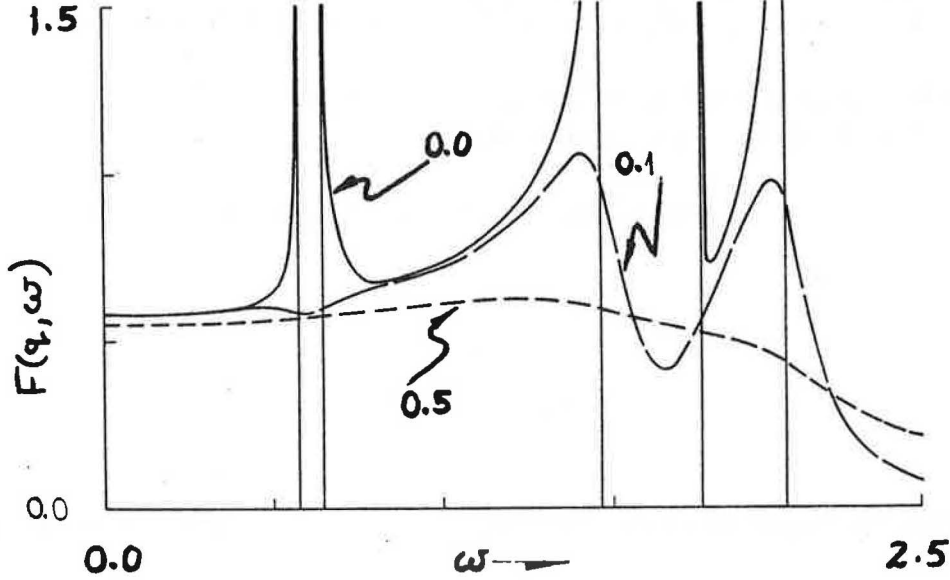


Fig. 4. The response function for transverse spin fluctuations in a longitudinally modulated magnet illustrating the influence of damping, with $\gamma = 0.0, 0.1$ and 0.5 as indicated. Other parameters are $N = 5$, $q = (\pi/4)$, $\beta = 0.15$ and $\alpha = -0.60 \cos(\pi/5)$.

The choice of sign for $\gamma \geq 0$ in complexification of the theory ensures that the poles of the propagator (Green function) occur only in the lower half-plane of the complex frequency. Introduction of a damping parameter is, of course, very familiar in quantum mechanics in the form of pole-avoidance. In the present context, it is worth mentioning that, $\gamma > 0$ ensures convergence of the temporal Fourier-Laplace transform of the casual Green function used in our formulation of the theory.

The appropriate prescription for the response function is relatively simple. Let us define

$$b(\omega) = b_1(\omega) + ib_2(\omega) = -L_N(\omega + i\gamma) , \quad (8.1)$$

and

$$a(\omega) = a_1(\omega) + ia_2(\omega) = B_{N-1}(\omega + i\gamma) . \quad (8.2)$$

Straightforward algebra then yields for the spectrum the following result,

$$\text{Im.}(a/\sqrt{b}) = (a_2 e_1 - a_1 e_2) \{b_1^2 + b_2^2\}^{-\frac{1}{2}}, \quad (8.3)$$

where

$$e_1 = (b_2 / 2e_2), \quad (8.4)$$

and

$$e_2 = \left\{ \frac{1}{2} \left[\sqrt{(b_1^2 + b_2^2)} - b_1 \right] \right\}^{\frac{1}{2}}. \quad (8.5)$$

Note that a_2 , b_2 and e_1 vanish in the limit $\gamma \rightarrow 0$. For e_1 and e_2 there is a common phase factor (± 1) not displayed in (8.4) and (8.5) about which we have more to say later.

The functions $b_1(\omega) = -L_N(\omega)$ and $a_1(\omega) = B_{N-1}(\omega)$ are derived by using the recursion relations provided in the previous section. It seems that the easiest way to find $b_2(\omega)$ and $a_2(\omega)$ is to expand $L_N(\omega + i\gamma)$ and $B_{N-1}(\omega + i\gamma)$ in γ ; $b_2(\omega)$ and $a_2(\omega)$ are polynomials in γ of order $(2N-1)$ and $(N-2)$, respectively. It is readily shown that approximating $b_2(\omega)$ and $a_2(\omega)$ by expressions correct to first-order in γ generates spurious effects in the response function. As a result of the dependence of b_2 and a_2 on γ and ω (and the external wave vector q) the contribution of the collision damping to the response function is non-trivial; an example is provided in Fig. (4).

The observed response function is, of course, a quantity which is necessarily positive or possibly zero. In our notation, the observed response function is proportional to $\{-\text{Im.}G(\omega)\}$. Now it is easy to show that (8.3) as a function of $\omega \geq 0$ is not of one sign. This feature is not a consequence of introducing collision damping, and it persists for $\gamma \rightarrow 0$. A positive result for $\{-\text{Im.}G(\omega)\}$ is related to the phase factor (± 1) common to e_1 and e_2 , which in turn is related to the convergence of the continued fractions in the formal solution for the propagator²⁷. For the present it suffices to say that the correct prescription for the phase of e_2 (and hence e_1) is that which renders $\{-\text{Im.}G(\omega)\}$ positive.

In the absence of damping ($\gamma = 0$) the observed response function ($L_N > 0$),

$$F(q, \omega) = -\text{Im.}G(\omega) / \omega = (\chi/2) |B_{N-1}(\omega)| \{L_N(\omega)\}^{-\frac{1}{2}} \quad (8.6)$$

considered as a function of frequency (ω) for a fixed wave vector (q), and N odd consists of N bands of intensity. The spectrum is symmetric about $\omega = 0$. An example is shown in Fig (4), while Fig. (3) shows $F(q, \omega)$ for $N = \text{even integer}$.

The undamped spectrum usually shows inverse square-root singularities at each band edge. It is possible with some special values of q to find the value zero at a band edge as in Fig. (3). This arises when as the band edge is approached $B_{N-1}(\omega)$ vanishes

with a power law dependence strong enough to cancel the square-root behaviour of the denominator. The finite value of the spectrum at $\omega = 0$ is a universal feature for modulated magnets.

Referring to Fig. (4), given that the maximum band edge frequency is 2.00 in our reduced units, a value of $\gamma = 0.10$ is viewed as a relatively small damping parameter. Even so we see in Fig. (4) that, such a damping has a pronounced effect on the spectrum. In particular, there is no vestige of the singular structure at the lowest two band edges (0.570 and 0.641), and the singular structure at 1.466 and 1.749 in the undamped spectrum are reduced to modest sized peaks.

Observe that there is next to no change in the magnitude of the spectrum at $\omega = 0$. Turning to results for a larger damping $\gamma = 0.5$, results in Fig. (4) show that the spectrum is reduced to a featureless landscape. Results for other parameter sets, including different values of the periodicity number N , show that results given in Fig. (4) are quite typical, in as much that a small damping profoundly effects low frequency structure found in the undamped spectrum and a modest damping removes most of the structure at all frequencies.

9. Acknowledgements

Some of the work discussed here has been accomplished with colleagues who include A. Cuccoli, E.B. Karlsson, V. Tognetti, K.N. Trohidou, G.I. Watson and D.R. Westhead.

10. References

1. J. Zinn-Justin, *Quantum Field Theory and Critical Phenomena*, (Oxford University Press, 1989).
2. K. Kawasaki and J.D. Gunton, *Progress in Liquid Physics*, ed. C. Croxton (Wiley, 1976).
3. H. Iro, *Z. Phys.* **B68** (1987) 485.
4. J.W. Cable and R.M. Nicklow, *Phys. Rev.* **B39** (1989) 11732, and *J. Phys.: Condens.Matter* **1** (1989) 7425.
5. D.C. Leslie, *Developments in the Theory of Turbulence*, (Clarendon Press Oxford, 1973).
6. S.W. Lovesey, *Condensed Matter Physics: Dynamic Correlations*, 2nd. Edition (Benjamin/Cummings, 1986).
7. A. Cuccoli, V. Tognetti and S.W. Lovesey, *Phys.Rev.* **B39** (1989) 2619.
8. A. Cuccoli, V. Tognetti and S.W. Lovesey, *J. Phys.: Condens.Matter* **2** (1990) 3339.

9. M.F. Collins, *Magnetic Critical Scattering*, (Oxford University Press, 1989).
10. C. Hohenemser, N. Rosov and A. Kleinhammes, *Hyperfine Int.* **49** (1989) 267.
11. M. Miasek, *Phys. Rev.* **107**, (1957) 92.
12. S.W. Lovesey, *Theory of Neutron Scattering from Condensed Matter*, Vol. 2, 3rd impression (Oxford University Press, 1987).
13. S.W. Lovesey, K.N. Trohidou, and E.B. Karlsson, *J. Phys.: Condens. Matter* **4** (1992) 2061.
14. U. Balucani, P. Carra, S.W. Lovesey, M.G. Pini, V. Tognetti, *J. Phys.* **C20** (1987) 3953.
15. E. Frey and F. Schwabl, *Hyperfine Int.* **50** (1989) 767.
16. S.W. Lovesey and R.D. Williams, *J. Phys.* **C19** (1986) L253.
17. C. Aberger and R. Folk, *J. de Physique* **C8** (1988) 1567.
18. See, for example, §15.5 in *Introduction to Phase Transitions and Critical Phenomena*, H.E. Stanley (O.U.P., 1971).
19. D.R. Westhead, A. Cuccoli, S.W. Lovesey and V. Tognetti, *J. Phys.: Condens. Matter* **3** (1991) 5235.
20. S. F. J. Cox. *J. Phys.* **C20** (1987) 3187.
21. E.K. Riedel, *J. Appl. Phys.* **42** (1971) 1383.
22. J. Als-Neilsen, *Phase Transitions and Critical Phenomena*, **5a** (1976) (Academic Press, London).
23. R. De Renzi. et al, *Phys. Rev.* **B30** (1984) 186.
24. M.P. Schulhof, P. Heller, R. Nathans, and A. Linz, *Phys. Rev.* **B1** (1970) 2304.
25. O. Hartmann et al., *Hyperfine Int.* **64** (1990) 369.
26. D.R. Hofstadter, *Phys Rev.* **B14** (1976) 2239.
27. S.W. Lovesey, *J. Phys.* **C21** (1988) 2805
and D.R. Westhead *J. Phys.: Condens. Matter*, **2**, (1990) 7407.
G.I. Watson, and D.R. Westhead, *Int. J. Mod. Phys.* **B5**, (1991) 1313.
28. P. van Moerbeke and D. Mumford, *Acta Math* **143** (1979) 93.

29. J.A. Blanco, D. Gignoux, and D. Schmitt, *Phys.Rev.***B45** (1992) 2529.
30. R.M. Nicklow and N. Wakabayashi, *Phys.Rev.* **B26** (1982) 3994.
31. C.J. Lantwin *Z.Phys.* **B79** (1990) 47.
32. H. Lin, M.F. Collins, T.M. Holden and W. Wei, *J.Mag and Mag.Materials* **104** (1992) 1511.

